Proceedings of the Reactor Physics Asia 2015 (RPHA15) Conference
Jeju, Korea, Sept. 16-18, 2015

Application of Source Expansion Nodal Method to SP3 Core Transient Analysis

Cheon Bo Shim[a], Jin Young Cho[a], and Han Gyu Joo[b,*]
[a]*Korea Atomic Energy Research Institute, 111, Daedeok-daero 989beon-gil, Yuseong-gu, Daejeon, 305-353, Korea*
[b]*Seoul National University, 1 Gwanak-ro, Gwanak-gu, Seoul, 151-744, Korea*
[*]Corresponding author: joohan@snu.ac.kr

1. Introduction

The development of high fidelity core simulators equipped with fast yet accurate numerical methods is one of the most significant research issues in the computational reactor physics area. Recently, the simplified P3 (SP3) method has been widely investigated to replace the diffusion (P1) method used in the conventional core simulators. While the P1 method approximates angular flux as a linear function of neutron angle cosine, the SP3 method considers the angular dependence up to the third order. And SP3 has an advantage that its equations are similar to the diffusion equation, so various established methods used in the diffusion simulators can be readily applied. One of them is the nodal method. It produces the spatial flux shape accurately in each computational node by using high-order functions. Thus there have been various studies to apply existing nodal methods to SP3[1-3] and it is proved that the SP3 nodal approach brings significant improvement in the prediction of neutronics behaviors, especially in severe spatial flux variation problems such as MOX loaded cores, small and/or fast reactors.

Although various outstanding nodal methods have been applied to SP3, however, most researches were limited to static neutronics analyses and there are only a few studies to apply the SP3 nodal in core transient analyses[4,5]. Furthermore, most of them adopted the Nodal Expansion Method(NEM). Because a fourth order polynomial based NEM has relatively poor accuracy compared to other advanced nodal methods such as the Analytic Nodal Method(ANM), Semi-Analytic Nodal Method(SANM), or Analytic Function Expansion Nodal(AFEN), it is worthwhile to apply such advanced methods to the time-dependent SP3 equations for high fidelity core transient analyses.

In this regard, this work is to apply a nodal method called Source Expansion Nodal Method(SENM)[3] to the time-dependent SP3 equations noting that the high accuracy of SP3 SENM have been already proved in steady-state analyses. In the next section, a brief description of the time-dependent SP3 SENM equations is presented. And the performance of the SP3 SENM is examined in the third section. The significance of this work is discussed in the conclusion.

2. Time-Dependent SP3 SENM Equations

General time-dependent multi-group SP3 equations can be represented as follow:

$$
\begin{aligned}
&\vec{\nabla}\cdot\vec{\phi}_{1,g}(\vec{r},t)+\left(\Sigma_{rg}(\vec{r},t)+\frac{1}{v_g}\frac{\partial}{\partial t}\right)\phi_{0,g}(\vec{r},t)\\
&=(1-\beta)\chi_{pg}\psi(\vec{r},t)+\sum_{k=1}^{6}\chi_{dgk}\lambda_k C_k(\vec{r},t)+\sum_{\substack{g'=1\\ g'\neq g}}^{G}\Sigma_{0,g'g}(\vec{r},t)\phi_{0,g'}(\vec{r},t)\\
&\frac{1}{3}\vec{\nabla}\phi_{0,g}(\vec{r},t)+\frac{2}{3}\vec{\nabla}\phi_{2,g}(\vec{r},t)+\left(\Sigma_{trg}(\vec{r},t)+\frac{1}{v_g}\frac{\partial}{\partial t}\right)\vec{\phi}_{1,g}(\vec{r},t)=0\\
&\frac{2}{5}\vec{\nabla}\cdot\vec{\phi}_{1,g}(\vec{r},t)+\frac{3}{5}\vec{\nabla}\cdot\vec{\phi}_{3,g}(\vec{r},t)+\left(\Sigma_{tg}(\vec{r},t)+\frac{1}{v_g}\frac{\partial}{\partial t}\right)\phi_{2,g}(\vec{r},t)=0\\
&\frac{3}{7}\vec{\nabla}\phi_{2,g}(\vec{r},t)+\left(\Sigma_{tg}(\vec{r},t)+\frac{1}{v_g}\frac{\partial}{\partial t}\right)\vec{\phi}_{3,g}(\vec{r},t)=0
\end{aligned}
\qquad (1)
$$

where $\phi_{m,g}(\vec{r},t)$ are the m^{th} moment of angular flux with m being 0 or 2 while the odd angular moments, $\vec{\phi}_{m,g}(\vec{r},t)$, are vectors with m being 1 or 3, and $\psi(\vec{r},t)$ is the total fission source. Compared to the static SP3 equations, Eq. (1) has only three different aspects. 1) The time dependency is considered. 2) The time-derivative of each angular moment appears in each moment balance equation. 3) The fission source is split to the prompt and delayed fission sources. In order to solve Eq. (1), the precursor density should be determined from the following precursor balance equation.

$$\frac{\partial C_k(\vec{r},t)}{\partial t}=\beta_k\psi(\vec{r},t)-\lambda_k C_k(\vec{r},t). \qquad (2)$$

In order to solve Eqs. (1) and (2), temporal discretization is required. Also each three-dimensional (3-D) equation is needed to be decoupled into three 1-D equations by the transverse integration and spatial normalization is required to apply SENM. In particular, the time-derivatives of each moment flux are treated as sources, and the total transient source is split to the static and transient specific sources (TSS). By applying them, Eq. (1) is reformulated as follow:

$$
\begin{aligned}
&\frac{2}{h_u}\frac{\partial}{\partial\zeta}\phi^i_{1u,g}(\zeta)+\Sigma^i_{rg}\phi^i_{0,g}(\zeta)=q^{ss,i}_g(\zeta)-q^{tl,i}_{0,g}(\zeta)+q^{ts,i}_{0,g}(\zeta)\\
&\frac{1}{3}\frac{2}{h_u}\frac{\partial}{\partial\zeta}\left(\phi^i_{0,g}(\zeta)+2\phi^i_{2,g}(\zeta)\right)+\Sigma^i_{trg}\phi^i_{1u,g}(\zeta)\\
&=-\frac{1}{v_g}\frac{\partial}{\partial t}\phi_{1u,g}(\zeta,t)\Big|_{t=t_i}\\
&\frac{1}{5}\frac{2}{h_u}\frac{\partial}{\partial\zeta}\left(2\phi^i_{1u,g}(\zeta)+3\phi^i_{3u,g}(\zeta)\right)+\Sigma^i_{tg}\phi^i_{2,g}(\zeta)\\
&=-\frac{2}{5}q^{tl,i}_{0,g}(\zeta)-\frac{3}{5}q^{tl,i}_{2,g}(\zeta)+q^{ts,i}_{2,g}(\zeta)\\
&\frac{3}{7}\frac{2}{h_u}\frac{\partial}{\partial\zeta}\phi^i_{2,g}(\zeta)+\Sigma^i_{tg}\phi^i_{3u,g}(\zeta)=-\frac{1}{v_g}\frac{\partial}{\partial t}\phi_{3u,g}(\zeta,t)\Big|_{t=t_i}\\
&\left(u=x,y,z\right)
\end{aligned}
\qquad (3)
$$

where i is time index for $t=t_i$ and

$$\zeta = \frac{2}{h_u}u, \left(-1 \le \zeta \le 1\right)$$
$$q_g^{ss,i}(\zeta) = \chi_g \psi^i(\zeta) + \sum_{\substack{g'=1 \\ g' \ne g}}^{G} \Sigma_{0,g'g}^i(\zeta)\phi_{0,g'}^i(\zeta),$$
$$q_{m,g}^{tl,i}(\zeta) = \sum_{\substack{u'=x,y,z \\ u' \ne u}} \frac{\phi_{(m+1)ur,g}^i(\zeta) - \phi_{(m+1)ul,g}^i(\zeta)}{h_{u'}},$$
$$q_{m,g}^{ts,i}(\zeta) = \delta_{0m}\left(\left(-\chi_g + (1-\beta)\chi_{pg}\right)\psi^i(\zeta) + \sum_{k=1}^{6} \chi_{dgk}\lambda_k C_k^i(\zeta) \right) - \frac{1}{v_g}\frac{\partial}{\partial t}\phi_{m,g}(\zeta,t)\Big|_{t=t_i}.$$
$$\left(m = 0,2\right)$$

In the conventional steady-state SP3 nodal approach, the SP3 equations are reformulated into two diffusion-like equations to apply nodal methods by representing the first and third moment fluxes as functions of the zeroth and second moments and by substituting them to the even moment balance equations. In the time-dependent equations, however, it cannot be done because of the time-derivative of the odd moments. In most existing time-dependent SP3 nodal studies, the odd moment time derivatives were neglected from the following assumption[5]:

$$\begin{aligned} \frac{1}{v_g}\frac{\partial}{\partial t}\vec{\phi}_{1,g}(\vec{r},t) &\ll \frac{1}{3}\vec{\nabla}\left(\phi_{0,g}(\vec{r},t) + 2\phi_{2,g}(\vec{r},t)\right) \\ \frac{1}{v_g}\frac{\partial}{\partial t}\vec{\phi}_{3,g}(\vec{r},t) &\ll \frac{3}{7}\vec{\nabla}\phi_{2,g}(\vec{r},t). \end{aligned} \tag{4}$$

If these assumptions are valid and the time-derivative of the odd moment fluxes can be neglected, the following diffusion-like SP3 equations can be derived.

$$-\frac{4}{h_z^2}\begin{bmatrix} D_{0,g}^i & 2D_{0,g}^i \\ \frac{2}{5}D_{0,g}^i & \frac{4}{5}D_{0,g}^i + \frac{3}{5}D_{2,g}^i \end{bmatrix}\frac{d^2}{d\zeta^2}\begin{bmatrix} \phi_{0,g}^i(\zeta) \\ \phi_{2,g}^i(\zeta) \end{bmatrix} + \begin{bmatrix} \Sigma_{rg}^i & 0 \\ 0 & \Sigma_{tg}^i \end{bmatrix}\begin{bmatrix} \phi_{0,g}^i(\zeta) \\ \phi_{2,g}^i(\zeta) \end{bmatrix} = \begin{bmatrix} q_g^{ss,i}(\zeta) - q_{0,g}^{tl,i}(\zeta) + q_{0,g}^{ts,i}(\zeta) \\ -\frac{2}{5}q_{0,g}^{tl,i}(\zeta) - \frac{3}{5}q_{2,g}^{tl,i}(\zeta) + q_{2,g}^{ts,i}(\zeta) \end{bmatrix} \tag{5}$$

where $D_{0,g}(t) = \frac{1}{3\Sigma_{trg}(t)}$ and $D_{2,g}(t) = \frac{3}{7\Sigma_{tg}(t)}$.

In the SENM, the intra-nodal flux shape is represented as the summation of two hyperbolic functions and a fourth order polynomial function.

$$\begin{aligned} \phi_{m,g}^i(\zeta) &= \phi_{m,g}^{H,i}(\zeta) + \phi_{m,g}^{P,i}(\zeta) \\ &= A_{m,g}^i \sinh(\kappa_{m,g}^i\zeta) + B_{m,g}^i \cosh(\kappa_{m,g}^i\zeta) + \sum_{l=0}^{4} c_{m,gl}^i P_l(\zeta) \end{aligned} \tag{6}$$

The coefficients of the particular solutions, $c_{m,gl}^i$, are determined from the coefficients of the fourth order static source $q_g^{ss,i}(\zeta)$ in which the contribution from the hyperbolic functions is approximated by a fourth order polynomial. The spatial shape of TSS is represented as a second order polynomial in the same way as the transverse leakage source (TLS).

$$\begin{aligned} q_g^{ss,i}(\zeta) &\simeq \sum_{l=0}^{4} s_{gl}^i P_l(\zeta) \\ q_{m,g}^{tl,i}(\zeta) &\simeq \sum_{k=0}^{2} l_{m,gk}^i P_k(\zeta) \\ q_{m,g}^{ts,i}(\zeta) &\simeq \sum_{l=0}^{2} b_{m,gl}^i P_l(\zeta) \quad (m = 0,2) \end{aligned} \tag{7}$$

The coefficients of the homogeneous solutions $A_{m,g}^i$ and $B_{m,g}^i$ are determined by the continuity conditions of the angular moments at each node interface and the two albedo boundary conditions. The determined analytic intra-nodal flux shapes are then expanded into a fourth order polynomial using the orthogonal property of the Legendre polynomial to update the source shape as:

$$\phi_{m,g}^i(\zeta) \simeq \sum_{l=0}^{4} \tilde{c}_{m,gl}^i P_l(\zeta) \tag{8}$$

The iteration to update the solution and source shapes ends when the fission source distribution converges sufficiently. All the detail information about the SP3 SENM method can be found in elsewhere[3].

3. Performance Examination

In order to demonstrate the effectiveness of the SP3 SENM in core transient analyses, two types of numerical analyses were performed. One was to examine the superiority of SENM compared to NEM in the SP3 solution and the other was to assess the improvement effects of SP3 in reactor kinetics. Each numerical analysis is covered in the following two sections.

3.1 Assessment of SENM in SP3

Because this work proposes SENM to be applied in the SP3 transient to resolve the limitation of the fourth order polynomial based NEM, it is necessary to compare the solutions of two nodal methods in SP3 core analyses. Prior to the transient comparison, their steady-state solutions are compared in a simplified 1-D problem derived from the C5G7 benchmark[6]. This problem consists of three assemblies of UO2, MOX, and reflector in sequence and 7-group XS data given in the benchmark are used. Table I shows the eigenvalue and reactivity error for the two SP3 nodal methods with various node sizes.

Table I. k-eff and its error in two SP3 nodal methods with various node sizes

Node Size	SP3 NEM	SP3 SENM
P_A	1.251061 (17.12)*	1.251377 (3.07)
$P_A/2$	1.251306 (1.47)	1.251331 (0.13)
$P_A/4$	1.251331 (0.13)	1.251329 (0.00)
$P_A/8$	1.251328 (0.06)	1.251329 (0.00)

* $e_\rho = \frac{1}{k_{eff,ref}} - \frac{1}{k_{eff}}$ (pcm); P_A: assembly pitch (=21.42 cm)

The reference was obtained by SP3 NEM with the node size of $P_A/16$. As noted in Table I, NEM has slightly

poorer accuracy in eigenvalue than SENM.

The inaccuracy of NEM comes from the fourth order polynomial based intra-nodal solution shape. The following figures show the NEM and SENM intra-nodal second moment shapes for Group 7 with the node sizes of P_A and $P_A/8$.

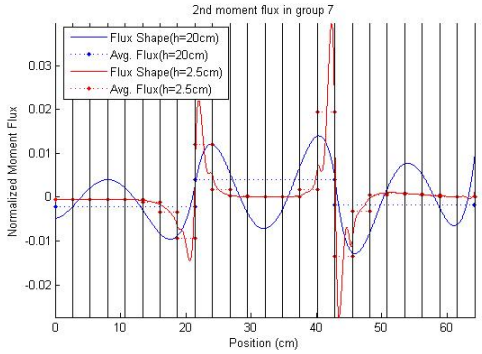

Fig. 1. NEM intra-nodal 2nd moment shape in Group 7.

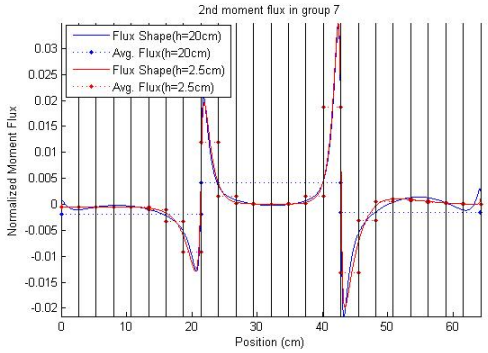

Fig. 2. SENM intra-nodal 2nd moment shape in Group 7.

It is clearly noted that the second angular moment is too steep especially at the node interfaces that NEM cannot predict it accurately whereas SENM shape is quite precise even for the larger node case.

The effectiveness of SENM in SP3 transient analyses was assessed with the NEACRP rod ejection accident (REA) benchmark[7]. Among the six accident scenarios of the PWR model, the A1 case was tested. Fig. 3 shows the core power behavior of the SP3 NEM and SENM for NEACRP A1 with various node sizes.

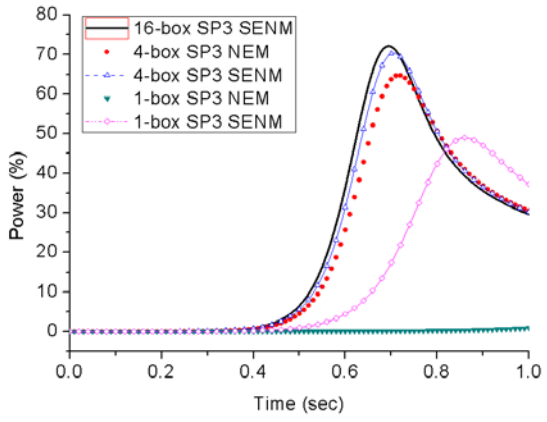

Fig. 3. SP3 NEM and SENM core power behaviors in NEACRP A1 with various node sizes.

These results confirm that SENM is much more accurate in the prediction of core power behavior than NEM. Especially, the 1-box NEM result is quite wrong.

Because the transient power variation mostly depends on the ejected rod worth in REAs, the control rod worth was estimated using the reactivities obtained for rod-in and rod-out states. Table II shows the result.

Table II. Rod worth and its error obtained by SP3 NEM and SENM in NEACRP A1 with various node sizes

Nodes/FA	SP3 NEM	SP3 SENM
1-box	755.2 (-40.2)	776.9 (-18.4)
4-box	789.2 (-6.1)	793.8 (-1.5)
16-box	N/A*	795.3 (0.0)

* 16-box SP3 NEM solution does not converge.

The 64-box SP3 SENM solution is used as the reference to obtain the errors. The 1-box SP3 NEM rod worth is estimated as 755.2 pcm and its error is 40.2 pcm. Because the total delayed neutron fraction β is 760 pcm in the NEACRP benchmark, the A1 case is predicted as a subprompt critical in the 1-box SP3 NEM calculation. It is why the flattened transient power occurred in Fig. 3. In safety analyses, it is significant to measure the severity of accidents and thus precise estimation of dynamic parameters is required. In this regard, NEM is not proper in the SP3 transient analyses unless the node size is sufficient small, but SENM is acceptable.

3.2 Assessment of SP3 effects in core transient analysis

The effectiveness of SP3 in transient is evaluated by comparing the diffusion and SP3 based NEACRP benchmark solutions. Fig. 4 shows the core power behavior of NEACRP A1 and B1 obtained by the diffusion and SP3 with the 4-box SENM nodal option.

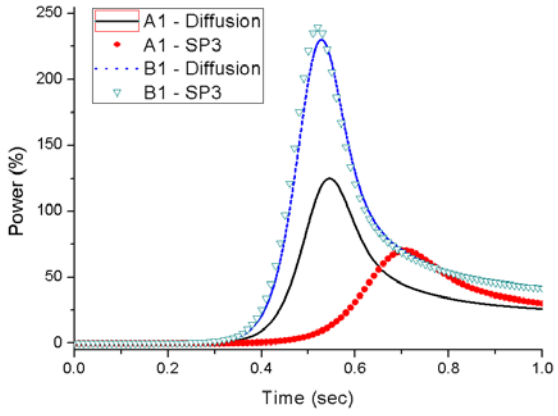

Fig. 4. Diffusion and SP3 core power behaviors in NEACRP A1 and B1.

While similar power behaviors are observed for the B1 case, the results for A1 are totally different. The reason for this difference is that A1 involves more heterogeneous initial condition for which the diffusion approximation suffers more due to severely rodded initial condition.

In order to clarify that, new cases of D1 and E1 were defined that they have same initial configuration of respective A1 and B1 with different ejected CR banks. Fig. 5 shows the core power behaviors of these cases.

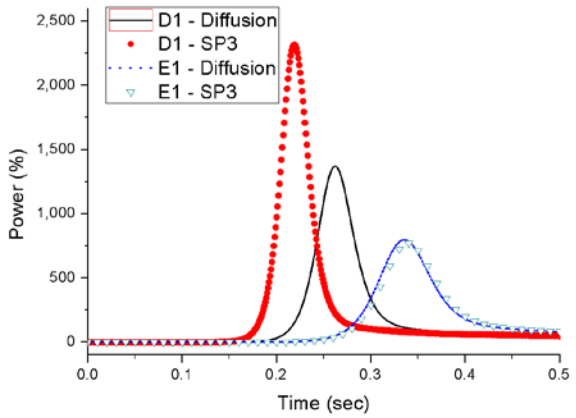

Fig. 5. Diffusion and SP3 core power behaviors in the new cases D1 and E1.

As noted in Fig. 5 that the D1 case shows more distinct power difference for the two methods whereas E1 shows similar transient power shape. This result proves that SP3 brings significant improvement in the computed neutron transient behavior particularly in problems where spatial flux varies severely.

In order to provide reference values for rod worth, the MOC based transport code nTRACER[8] is used. Because it is enough to compare the ejected rod worth instead of the transient solutions to assess the SP3 effect in transient analyses, simplified 2-D NEACRP cases were solved. The 2-D core configurations are defined as the midplane of the 3-D problems. Table 3 shows the k-eff of the rod-in and rod-out states and the estimated rod worths obtained by each method in the 2-D NEACRP A1 and B1 cases.

Table 3. k-eff in the rod-in and rod-out states and the estimated rod worths in 2-D A1 and B1

Case	Solver	k-eff in Rod-in	k-eff in Rod-out	Rod worth (pcm)
A1	Transport	1.04411	1.05383	883.38
	Diffusion	1.04269 (-130.4)	1.05262 (-109.1)	904.74 (21.4)
	SP3	1.04410 (-0.9)	1.05382 (-0.9)	883.40 (0.0)
B1	Transport	1.12024	1.12975	751.43
	Diffusion	1.11935 (-71.0)	1.12884 (-71.4)	751.05 (-0.4)
	SP3	1.12022 (-1.6)	1.12972 (-2.4)	750.67 (-0.8)

It is clearly noted that the SP3 solutions are very close to the reference whereas the diffusion results have nontrivial errors. From these results, it is demonstrated that SP3 is required for high fidelity core transient analyses.

4. Conclusions

In this work, the SENM nodal method was extended to the time-dependent SP3 equations for high fidelity core transient analyses. The intra-nodal shapes of both zeroth and second angular moments were represented as the SENM hyperbolic and fourth order polynomial functions.

Owing to the hyperbolic functions used in SENM, the drastically changing second moment shapes can be predicted accurately and it leads to much improved results for neutronics behavior analysis whereas it is unable with the SP3 NEM. The SP3 applications to the core transient analysis also offer considerable enhancements in the transient power prediction over the conventional diffusion approach. It is particularly remarkable in the cores where proper consideration of the significant transport effect is required because of severe spatial material and flux variation. In this regard, it is demonstrated that the developed time-dependent SP3 SENM method can be used effectively in high fidelity transient core simulations.

References

1. Lee C. H. and Downar T. J, ‘‘A Hybrid Nodal Diffusion/SP3 Method Using One-Node Coarse-Mesh Finite Difference Formulation,” *Nucl. Sci. Eng.*, **146**, 176 (2004).
2. Beckert C, and Grundmann U, “Development and Verification of a Nodal Approach for Solving the Multigroup SP3 Equations,” *Ann. Nucl. Energy*, **35**, 75 (2008).
3. Jeong H. J, “Alternating Direction One-Dimensional Source Expansion Nodal Method for Whole Core Simplified P3 Calculation,” M.S. Thesis, Seoul National University (2013).
4. Lee C. H, Kozlowski Tomasz, and Downar T. J, “Analysis of Control Rod Ejection Accident in MOX and MOX/UOX Cores with Time-Dependent Multigroup Pin-by-Pin SP3 Methods,” *Proc. PHYSOR 2002*, Seoul, October 7-10, 2002, American Nuclear Society (2002) (CD-ROM).
5. Lee D. J, Kozlowski Tomasz, and Downar T. J, “Multi-Group SP3 Approximation for Simulation of a Three-Dimensional PWR Rod Ejection Accident,” *Ann. Nucl. Energy*, **77**, 94 (2015).
6. Lewis E. E. et al., ‘‘Benchmark Specification for Deterministic 2-D/3-D MOX Fuel Assembly Transport Calculations without Spatial Homogenization (C5G7MOX),’’ NEA/NSC/DOC (2001)4, OECD Nuclear Energy Agency (2001).
7. Finnemann H. and Galati A, “NEACRP 3D LWR Core Transient Benchmark Final Specification,” NEACRP-L-335 (Rev. 1), Nuclear Energy Agency Committee on Reactor Physics (1992).
8. Jung Y. S. et al., “Practical Numerical Reactor employing Direct Whole Core Neutron Transport and Subchannel Thermal/Hydraulic Solvers,” *Ann. Nucl. Energy*, **62**, 357 (2013).